1

Upgrading of Biomass via Catalytic Fast Pyrolysis (CFP)

Charles A. Mullen

USDA-Agricultural Research Service, Eastern Regional Research Center, 600 E. Mermaid Lane, Wyndmoor, PA, USA

1.1 Introduction

Defined as heating of an organic material in a nonoxidative environment, pyrolysis has been recognized for decades as the most efficient process for converting lignocellulosic biomass into a dense liquid, commonly called *pyrolysis oil* or *bio-oil* [1–3]. The most commonly used conditions for conversion of biomass to liquid have been high heating rates to temperatures of around 500 °C, at atmospheric pressure, the so-called fast pyrolysis process [1–3]. The fast pyrolysis process offers many advantages that make it attractive for conversion of biomass to bio-fuel intermediates and production of renewable chemicals. These advantages include high liquid yields (>60% in some cases) and production of a potentially valuable coproduct in *bio-char*. This solid, consisting of fixed carbon and minerals, has been shown to be a good soil amender and a potential route to sequester carbon [4–6]. With the potential utilization of the combustible off gases, and if needed some of the bio-char, pyrolysis can be powered by its own energy, making it a nearly self-sufficient process requiring few other inputs [3].

Bio-oil contains hundreds of oxygenated compounds derived from the cellulose, hemicellulose, and lignin that comprise the biomass. In recent years, much has been made of bio-oil as a potential intermediate to the production of advanced hydrocarbon transportation fuels or as a feedstock from which to isolate renewable chemicals. However, commercial or even precommercial success for utilization of these bio-oils has been limited to lower value applications such as use as boiler-type fuels for heat and power [3, 7] or utilization as an asphalt-like material [8]. The technical reason for these limitations is that the composition of the bio-oil, comprising high concentrations of reactive oxygenated functional groups, plus the presence of catalytic microsolids, makes the mixture thermally unstable [9–11]. Therefore, processing technologies requiring even moderate heating of the bio-oil mixture, such as distillation, result in production of intractable materials [12]. While catalytic hydrodeoxygenation (HDO) has been the post-production upgrading choice for refining of bio-oil to hydrocarbons to be used as fuels, the unstable nature of the bio-oil also makes

Chemical Catalysts for Biomass Upgrading, First Edition. Edited by Mark Crocker and Eduardo Santillan-Jimenez.

this HDO process difficult. The most effective post-production deoxygenation processes developed require multiple catalytic, high pressure hydrotreating steps, at significant cost, making the production of a low margin fuel product of questionable economic viability [13–15].

Because of these limitations, researchers have sought to develop processes that alter the chemical pathways during pyrolysis to produce a more stable bio-oil product with more favorable compositions for various end-use applications, including HDO. Utilization of heterogeneous catalysts during the pyrolysis process, termed *catalytic fast pyrolysis* (CFP), has received the most attention. Because of the interest in advanced hydrocarbon bio-fuels, the most common goal of catalytic pyrolysis has been to produce a partially deoxygenated, thermally stable pyrolysis oil that is more amenable to final HDO-type upgrading to fuel-range hydrocarbons. However, alternative processes have aimed to converge chemical pathways toward production of various individual compounds or groups of compounds for petrochemical or fine chemical uses. In this chapter we will discuss CFP processes both aimed at general deoxygenation and those aimed at targeted classes of molecules. For the purposes of this chapter, we will consider catalytic pyrolysis processes that fall within the following definitions: (i) heterogeneous catalytic processing of biomass pyrolysis vapors either *in situ* (pyrolysis and catalysis occur in the same reactor zone) or *ex situ* (pyrolysis and vapor phase catalysis are decoupled) and (ii) reactions taking place in inert or reactive (but non-oxidative) atmospheres at near atmospheric pressure. Therefore, catalytic hydrothermal or solvent liquefaction [16] and other technologies such as pressurized hydropyrolysis [17] are outside the scope of this chapter.

As mentioned earlier, CFP encompasses processes where solid biomass contacts the catalyst and both pyrolysis and vapor upgrading occur in the same reactor, the so-called *in situ* methods, and processes where the pyrolysis and catalytic vapor upgrading occur in separate reactors, called *ex situ* or *vapor upgrading* methods. Simplified schematics of the two processes are presented in Figure 1.1. The main advantage of the *in situ* method is its simplicity – the "one-pot" reaction system saves capital cost as it does not require a second reactor. However, there are several advantages that decoupling the two steps allows for [18]. While it is well known that temperatures in the 500 °C range produce the maximum yield of condensable range species from pyrolysis of most biomass, the ideal range for various catalytic processes may be significantly different, depending on the catalyst and the desired end products. Furthermore, because the *in situ* process requires contact of solid biomass with solid catalyst, reactors for the unit operation tend to be limited to only fluidized beds. Decoupling the process allows the catalysis step to occur in either a fixed or fluidized bed and also allows for other various reactor types to accomplish the pyrolysis. Another very important factor is that the *ex situ* process allows for removal of bio-char and its associated metal content prior to introduction of the catalyst. This has important implications for catalyst lifetimes as inorganic materials contained in the biomass, particularly Group 1 and Group 2 metals, can poison catalysts, leading to more frequent catalyst replacement or replenishment and a higher catalyst demand. This is an especially important consideration for zeolite-catalyzed processes because they are highly susceptible to this type of deactivation, as described later.

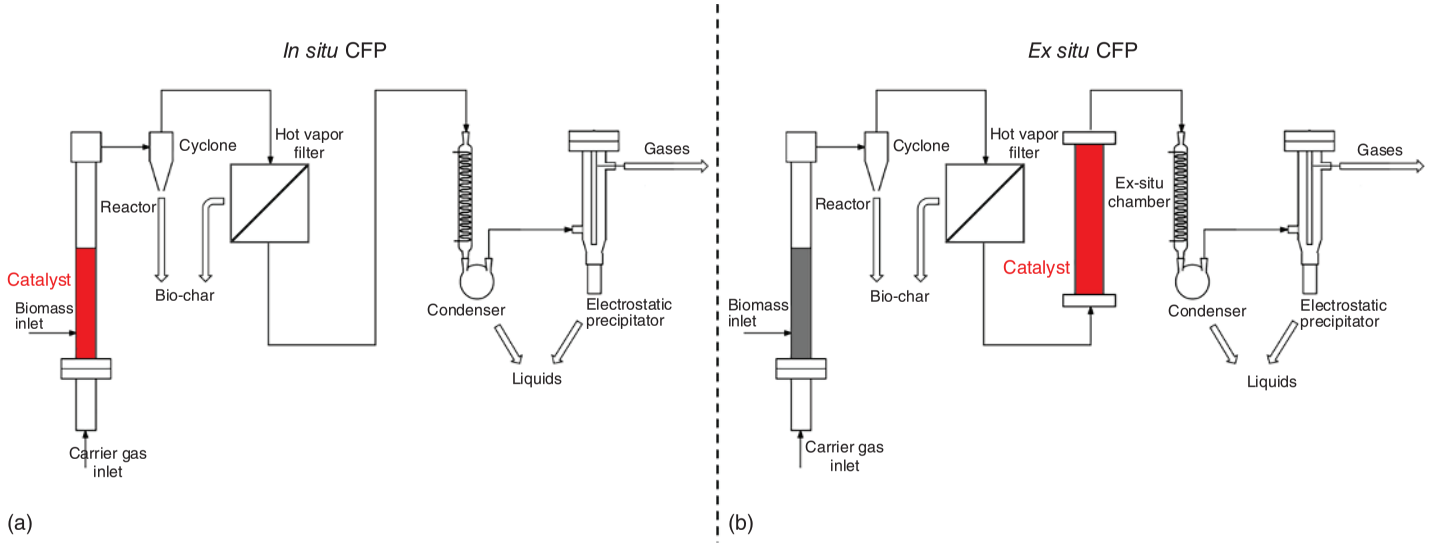

Figure 1.1 Simplified process schematics comparing (a) *in situ* and (b) *ex situ* catalytic pyrolysis.

1.1.1 Catalytic Pyrolysis Over Zeolites

Zeolites and similar materials have been by far the most common catalysts employed in CFP processes. Zeolites are crystalline substances with a structure characterized by a framework of linked tetrahedra, each consisting of four oxygen atoms surrounding a cation [19–21]. Zeolites occur naturally, but the advent of synthetic zeolites in the 1950s, free of the defects and impurities found in nature, is when their use in chemical catalysis took off [20]. Industrial scale catalytic use of zeolites started in 1962, with the use of zeolites X and Y for fluid catalytic cracking (FCC) of heavy petroleum fractions, a process that is still today one of the highest volume chemical processes used. Other petrochemical uses include hydrocracking, isomerization, disproportionation, and alkylation of aromatics. The framework of zeolites is usually silica and alumina based. This framework contains open cavities in the form of channels and cages [19]. These are usually occupied by H_2O molecules and extra-framework cations that are commonly exchangeable [19]. In silica–alumina-based materials, the need for the extra-framework cation is to balance the charge imbalance created by the four coordinate Al(III) sites, as opposed to the neutral Si(IV) sites (Figure 1.2) [19–21]. Often, in the active catalysts, some or all of the extra-framework cations are Brønsted acid (H^+) active sites, which along with the Lewis acidity of other sites are responsible for initiating the catalytic reactions. The channels allow the passage of guest species to these active sites [19–21]. In biomass CFP these guest species are molecules derived from the breakdown of the biopolymers caused by the initial pyrolysis reactions. The pore size and shape, Brønsted acid strength and site density, and the presence of other types of active sites are important factors in the activity and selectivity of the catalysts.

1.1.1.1 Catalytic Pyrolysis Over HZSM-5

Several different types of zeolites have been tested as catalysts for the deoxygenation of pyrolysis vapors including Zeolite Socony Mobil-5 (ZSM-5), Y, beta, mordenite, and ferrierite [22–26]. Among these types of zeolites, the ZSM-5 (also called MFI for mordenite framework inverted)-based materials have shown the most promise and received the most attention and will be the focus of this section. ZSM-5-type zeolites have been shown to selectively convert molecules from a wide variety of sources to aromatic hydrocarbons. Among these processes are methanol to olefins and gasoline and cracking of waste hydrocarbon plastics [27, 28]. Aromatic hydrocarbons are good target product molecules from biomass, because, like the biomass starting materials, they have low H/C ratios, meaning the biomass carbon can be more efficiently converted without the

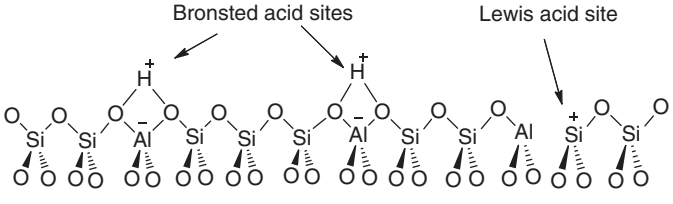

Figure 1.2 Brønsted and Lewis acid sites of zeolites.

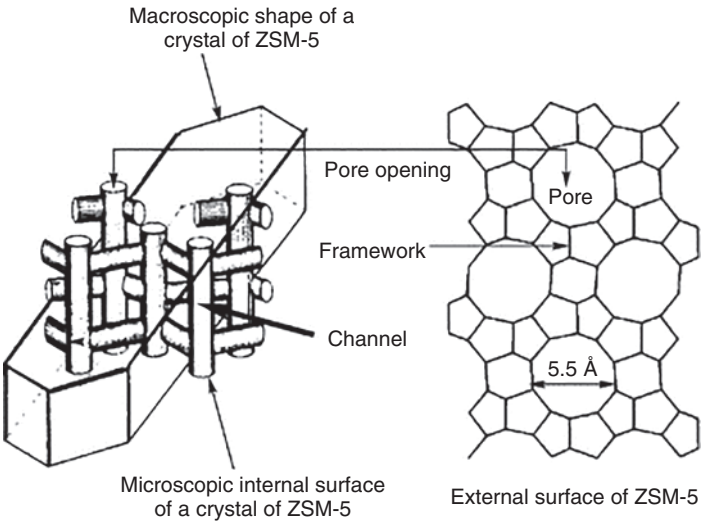

Figure 1.3 Structure of ZSM-5. Source: Lei et al. 2003 [30]. Reproduced with permission of Royal Society of Chemistry.

addition of an external source of hydrogen [29]. The shape selectivity of ZSM-5 is responsible for convergence toward aromatics. ZSM-5 has a three-dimensional pore system comprising straight 10-membered ring 5.2×5.7 Å channels connected by sinusoidal 5.3×5.6 Å channels (Figure 1.3) [25, 30]. This puts it in the category of a medium pore size zeolite. This pore structure creates a mass transfer effect, limiting the molecules that enter and interact with the chemical functionality of the acid site based on size. At the same time, the confined space limits the geometry that can occur in the reaction transition states, forcing the chemistry through certain pathways, creating the observed product selectivity [24].

Biomass catalytic pyrolysis, whether the physical process is performed in the *in situ* or *ex situ* configuration, encompasses two distinct chemical processes. First, pyrolytic decomposition of the biopolymers produces oxygenated vapors, aerosols, and bio-char. The catalyst is involved in the second step wherein some of the oxygenated gas phase products interact with the catalyst, initiating reactions that alter the composition of the gas stream and hence the condensed product that is collected. The various oxygenated pyrolysis products that are the substrates in the catalytic reactions have differing interactions with the catalyst, depending on several factors including whether their molecular size allows entry into the pores of the catalyst, their diffusion rate through the channels, and the interaction of their chemical functionality with the catalyst active site and other reactants present. During catalytic pyrolysis over HZSM-5, most of the aromatic hydrocarbons are ultimately derived from the carbohydrate portions (cellulose and hemicellulose) of the biomass, while lignin-derived vapors are considered primarily, but not entirely, as precursors to coke formation [30, 31]. The portions of the lignin that do contribute to the hydrocarbon pool are mostly derived from the carbon chain linkers or side chains rather than the phenolic units themselves [32]. The chemical pathways that occur to produce aromatic hydrocarbons are summarized in Figure 1.4. The key step after production of oxygenated vapors

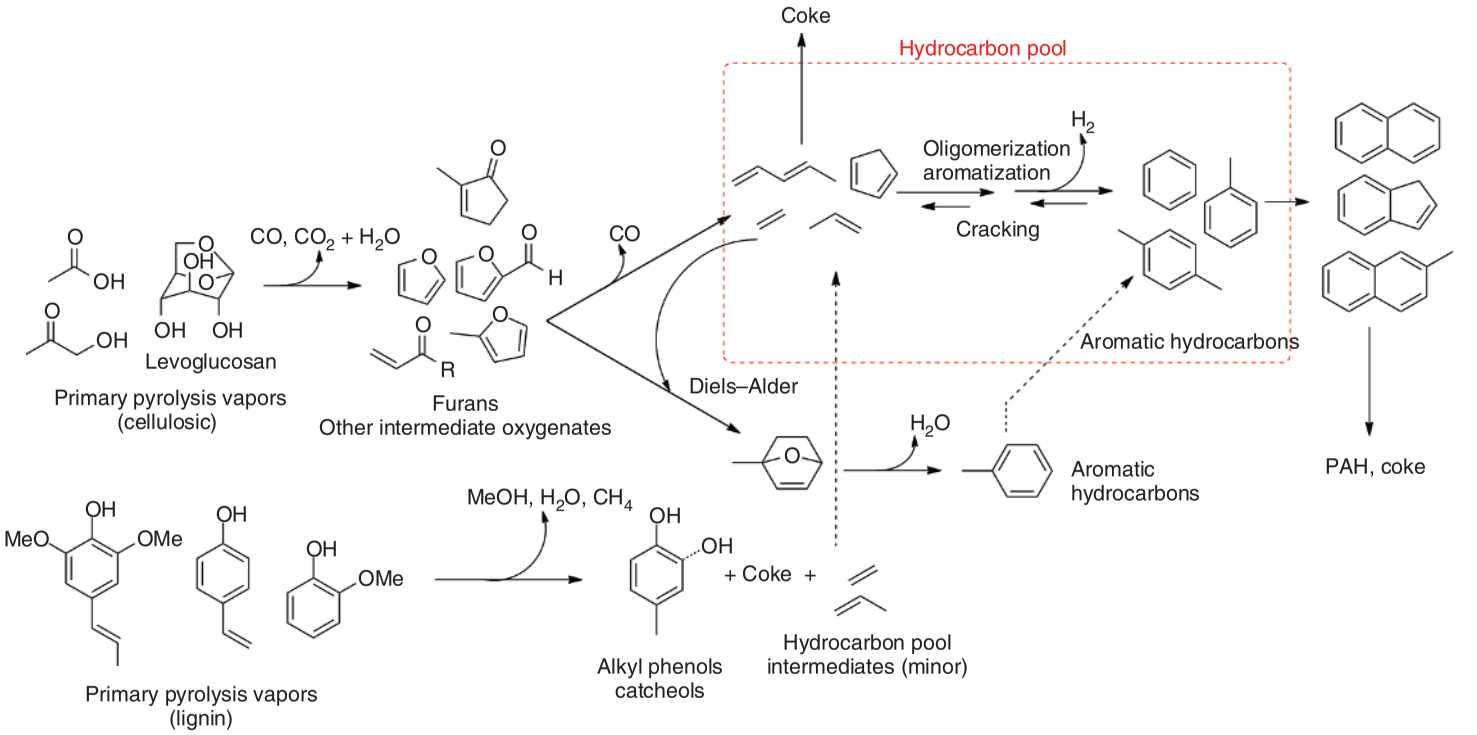

Figure 1.4 Major chemical pathways from primary pyrolysis vapors to aromatic hydrocarbons via CFP over HZSM-5.

via the initial pyrolytic depolymerization is the dehydration of compounds such as anhydrosugars to form furans [33]. This step can occur on the surface of the catalysts, producing smaller molecules that can diffuse into the micropores [25, 34, 35]. Here, two main pathways toward aromatics become operative. The first pathway involves decarbonylation to form olefins which can go on to oligomerize and aromatize. This mixture of olefins and product hydrocarbons is referred to as the *hydrocarbon pool* [33]. Alternatively, Diels–Alder-type cycloaddition reactions of furans with olefins can directly produce aromatics upon dehydration of the bicyclic cycloaddition adduct [36]. Related reactions of other primary pyrolysis products can also produce CO_2 along with olefins and alkanes.

Many studies have been conducted on the effects of process conditions for catalytic pyrolysis of biomass and their components over HZSM-5, focused either on the goal of producing partially deoxygenated bio-oil (for direct bulk use or further processing), or for the production of aromatic hydrocarbons and light olefins [22–26, 29, 37–49]. An estimated carbon balance for CFP of biomass over HZSM-5 is presented in Figure 1.5 [49], and Table 1.1 summarizes the details of selected studies where product samples were produced (i.e. larger than analytical or micropyrolyzer studies). While there are many factors that contribute to the variation in the reported results, generally the level of deoxygenation achieved follows an inverse trend with bio-oil yield [50]. Lower biomass to catalyst ratios, corresponding to higher catalyst activity, result in more deoxygenation at the expense of bio-oil yield; potential organic liquid yield is lost to gas phase products, water, and coke [18, 49]. While overall organic liquid yield decreases due to elimination of oxygenated species, yields of aromatic hydrocarbons generally increase with increasing biomass to catalyst ratio. Residence time and space velocity considerations can also affect the conversion to aromatic hydrocarbons. In a study on CFP of cellulose over HZSM-5 in an *in situ* fluidized bed process, at equal weight hourly space velocity (WHSV), a gas residence time of about 8.6 seconds (studied over a range of 5.6 to ~10 seconds by changing carrier gas flow rates) maximized aromatic yield [46]. Selectivity for benzene and toluene were also maximized at this residence time, while selectivity to xylenes and naphthalenes was minimized.

As mentioned earlier, the cellulosic portion of the biomass is most efficiently converted to aromatic hydrocarbons, while only a small portion of lignin can be converted to aromatic hydrocarbons over HZSM-5. A number of other factors related to the biomass composition can also affect the production of aromatics. This gives rise to variation in yields and quality of liquid products and aromatic hydrocarbons. Biomass composition, along with process conditions and catalyst properties are also important variables in catalyst deactivation rates, which are discussed in detail later. Studies of biomass within a small range of compositions have found, unsurprisingly, that increased ash content (particularly potassium) correlates with decreased conversion of carbon to aromatics during CFP, due to an increased production of gases, and increased lignin is also correlated with decreased aromatics and increased coke yield [51].

With regards to the properties of a standard HZSM-5 zeolite catalyst that influence biomass vapor upgrading, the number of Brønsted acid sites the biomass is exposed to, controlled by the acid site density (inversely proportional to the

Table 1.1 Selected results of biomass CFP over typical HZSM-5 catalysts.

Biomass	Scale (kg/h)	Configuration	SAR[a)]	Temperature (°C)	C/B (mass)	WHSV[b)](h^{-1})	Bio-oil yield (C%)[c)]/oxygen content (wt%)	AHC[d)] yield (C%)[c)]	References
Cellulose	~0.06	*In situ*	30	500		0.25	—	39.5	[46]
Lignin	mg	*In situ*[e)]	23	650	15		—	8.2	[32]
Pine	~0.165	*In situ*	30	600	6	0.3		15.5	[43]
Pine	2	*In situ*	—	475	0.33	2	13.3/19.42		[45]
Hybrid poplar	2	*In situ*	—	475	0.33	2	12.2/20.25		[45]
Corn stover	2	*In situ*	—	475	0.3	2	8.9/13.99		[45]
Switchgrass	2	*In situ*	—	475	0.33	2	15.8/14.7		[45]
Juniper	2	*In situ*	—	475	0.33	2	15.8/12.3		[45]
Pine bark	2	*In situ*	—	475	0.33	2	8.9/18.9		[45]
Switchgrass	0.3	*In situ*	30	450–500	0.5	1.2	9.4/23.5		[41]
Corn cob	0.036	*In situ*	48	550	5		25.5/14.69		[38]
Pine wood	20	*In situ*	50	550	7		24/21.5		[42]
Beech wood	0.5	*In situ*	50	500	11		27/19.5		[47]
Beech wood	0.5	*In situ*	50	500	21		23/17.5		[47]
Pine	0.150	*Ex situ*	30	500	2		14.3/4.0		[48]
Pine	0.150	*Ex situ*	30	500	0.67		17.2/14.2		[48]
Pine	0.150	*Ex situ*	30	500	0.48		23.1/17.7		[48]

a) SAR, silica alumina ratio.
b) WHSV, weight hourly space velocity.
c) C%, carbon yield.
d) AHC, aromatic hydrocarbons.
e) Micropyrolyzer.

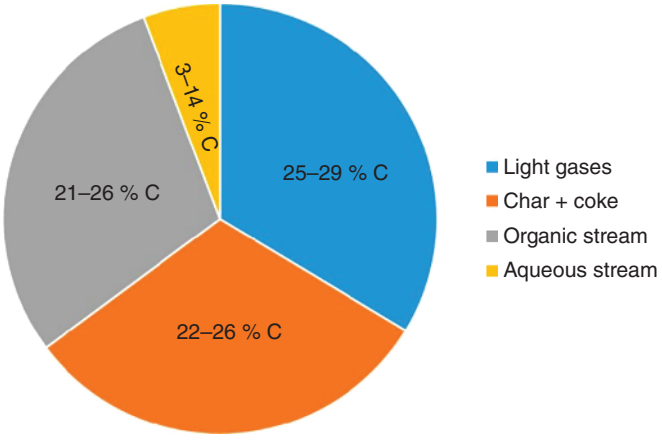

Figure 1.5 Typical carbon distribution from CFP of biomass over HZSM-5 and related catalysts. Source: Starace et al. 2017 [49]. Reproduced with permission of American Chemical Society.

silica/alumina ratio) is the most important variable controlling activity [40], along with the biomass to catalyst ratio. In the absence of other variations, the higher the acid site density, the more active the catalyst. This generally leads to higher yields of aromatics; however, at very high acid site densities, the small distance between active sites can promote the formation of coke, decreasing the initial yield of aromatic hydrocarbons and also leading to more rapid catalyst deactivation as discussed in more detail in the succeeding text [52]. One study looking at aromatic hydrocarbon yields when using HZSM-5 with $SiO_2/Al_2O_3 = 23$, 30, 50, and 80, found 30 as the optimum to maximize the yield of aromatic hydrocarbons [40]. Lower SiO_2/Al_2O_3 also correlated with higher production of CO_2 (but not CO), indicating Brønsted acid dependence for any decarboxylation reactions, although this is a relatively minor deoxygenation pathway in CFP over zeolites. High acidity also increased selectivity for benzene and toluene over C8+ aromatics including xylenes, ethyl benzene, and indanes [40].

1.1.1.2 Deactivation of HZSM-5 During CFP

Catalyst deactivation is a significant concern for biomass CFP. Zeolites are subjected to three major deactivation mechanisms during the process. The first is formation of coke that blocks access to the catalyst active site. This is the most rapid form of catalyst deactivation and can have noticeable effects on the product distribution almost immediately at cumulative biomass/catalyst mass ratios of <1. Fortunately, this type of deactivation is also reversible, via combustion of the coke. A second form of deactivation results from poisoning of the catalyst active sites with inorganic species from the biomass, particularly alkali metals. This type of deactivation is, for practical purposes, irreversible. A third type of deactivation is physical degradation of the catalyst, most commonly dealumination. This can occur due to exposure to high temperatures and steam and can also occur during combustion process used to regenerate catalysts from coke deposits. This type of deactivation is also irreversible.

There are two main mechanisms of coke formation active during biomass CFP. The first is similar to coke formation that occurs during other zeolite catalyzed reactions (including petroleum processing and methanol to olefins), i.e. molecular weight growth of already formed aromatics by reaction with other aromatics or olefins present in the hydrocarbon pool [50, 53]. Because biomass pyrolysis vapors are deficient in hydrogen, any deoxygenation occurring by dehydration reactions will further reduce the hydrogen content of the vapors favoring molecular weight growth reactions that form large aromatic molecules with low H/C ratios that comprise coke. This process can be further exacerbated by slow diffusion of products out of the zeolite [25]. Another source of coke is direct condensation or deposition of lignin-derived phenolics, which have poor reactivity over ZSM-5 and tend to be too bulky to navigate the pores of the catalyst [54]. If HZSM-5 catalysts are not regenerated by combustion of the coke, complete deactivation of the catalyst and production of product vapors with similar oxygen content and composition to noncatalytic pyrolysis are produced at cumulative biomass to catalyst ratios of about 3 or 4 to 1 for biomass such as wood and grasses [50, 55, 56]. Lignin deactivates catalysts much quicker than cellulose and use of feedstocks with high lignin concentration may result in more rapid catalyst deactivation via coking. The rapid coking effect can account for a significant portion of the variability in results and the effect of biomass to catalyst ratios as seen in Table 1.1, depending on run lengths and regeneration protocols.

The effect of coking on the product vapors can be seen almost immediately, at very low cumulative biomass to carbon ratios. During CFP over HZSM-5, the first oxygenates to appear are not primary pyrolysis vapors but partially deoxygenated species including furans, phenols, and alkyl phenols (mostly cresols) [50]. Furans are intermediates on the pathway from anhydrosugars (cellulose primary pyrolysis products) to aromatics, and their appearance is reflective of the loss of catalytic activity for the decarbonylation step that results in their conversion to olefins that make up part of the hydrocarbon pool (see Figure 1.4). A decrease in CO formation has been observed to occur at low cumulative/biomass ratios [56]. Phenols have also been found as a partially deoxygenated product from both cellulose and lignin [51, 55–57]. Unlike furans, phenols are not intermediates on the pathway from cellulosic primary pyrolysis vapors to aromatic hydrocarbons. There is evidence that they are formed via a reaction of deoxygenated species still bound to the catalyst with water, confirmed by observing the incorporation of ^{17}O in phenolic products from labeled water added in a CFP experiment [57]. These products of partially deactivated catalysts reach a maximum and then begin to become less concentrated as the activity for even the initial dehydration step becomes nullified by coke blocking both internal and surface acid sties [50]. Primary pyrolysis products are then observed at higher cumulative biomass/catalyst ratios. The product vapors consist of a mixture of the three groups until the complete deactivation point is reached. The results of one study monitoring the composition of the vapors over the course of CFP up to a cumulative biomass to catalyst ratio of 4.5/1 is presented in Figure 1.6 [50].

Coking rates can vary with catalyst properties, particularly with acid site density. As discussed earlier, the activity of fresh catalysts generally trends with Brønsted acid site density, but yields of aromatic hydrocarbons were

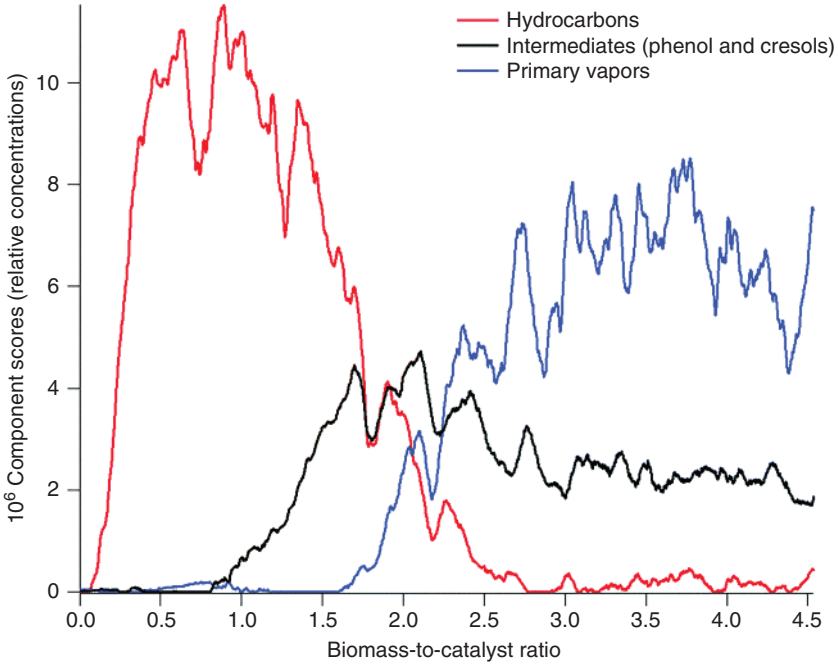

Figure 1.6 Trends in concentration of aromatic hydrocarbons, intermediate products from pine pyrolysis over HZSM-5 (microreactor-MBMS system) vs. cumulative biomass to catalyst ratio. Source: Mukarakate et al. 2014 [50]. Reproduced with permission of Royal Society of Chemistry.

optimized at $SiO_2/Al_2O_3 = 30$ over an even more acid-site-dense catalyst with $SiO_2/Al_2O_3 = 23$ [40]. The reason for this is likely a more rapid deactivation of the more acidic catalyst due to increased coking over the short course of the experiment. One study, which decoupled activity and deactivation from the total number of acid sites, found that HZSM-5 with a SiO_2/Al_2O_3 of 40 had comparable initial activity for the production of aromatic hydrocarbons, but the deactivation rate was significantly slower than catalysts with higher acid site density (Figure 1.7) [52]. Some studies on model compounds have shown that close proximity of acid sites can facilitate the condensation (C—C bond and H_2O forming) reactions between oxygenated intermediates, leading to coking [52, 58]. A change in the amount of extra-framework alumina, which can serve as nucleation sites for molecular weight growth, can also lead to coking. In the following Sections 1.1.3 and 1.1.4 that discuss modification of HZSM-5, the effects of various changes to the catalyst structure with respect to deactivation are considered.

Alkali metals present in the biomass are also a problematic source of catalyst deactivation. Alkali metals can accumulate on catalysts rapidly and can ion exchange with Brønsted acid sites, deactivating the sites. In two studies of *in situ* CFP over HZSM-5 (where catalysts were regenerated from coking, one by use of a circulating fluidized bed and one by intermittent regeneration) mineral

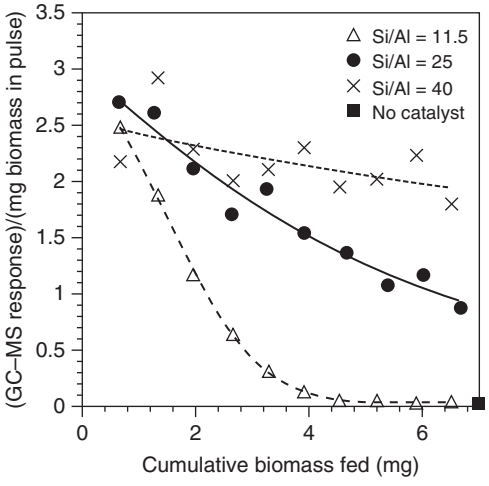

Figure 1.7 Comparison of alkylbenzenes production on HZSM-5 Si/Al = 11.5, 25, and 40 from oak pyrolysis vapors with fixed total sites at 500 °C. Source: Wan et al. 2015 [52]. Reproduced with permission of John Wiley and Sons.

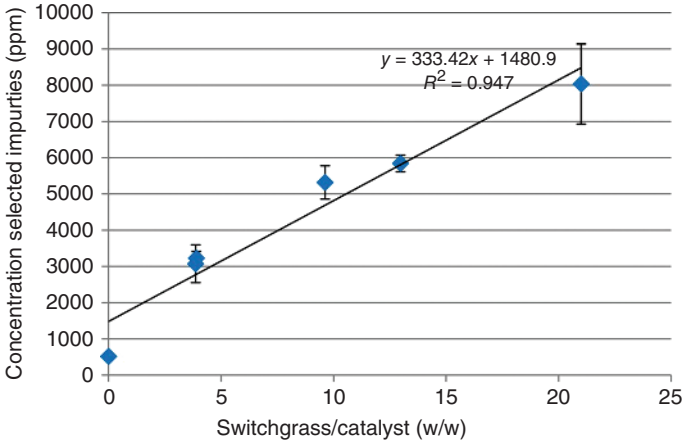

Figure 1.8 Concentration of total Ca, Cu, Fe, K, Mg, Na, and P on HZSM-5 at different levels of catalyst exposure to switchgrass in a fluidized bed at pyrolysis conditions (500 °C, N_2). Values are the average of three inductively coupled plasma spectroscopy (ICP) measurements. Error bars are one standard deviation. Source: Mullen and Boateng 2013 [41]. Reproduced with permission of American Chemical Society.

accumulation including Ca, K, Mg, Na, and P was found to be linear with time on stream (or cumulative biomass/catalyst ratio) [41, 42]. Each study, one with switchgrass (~2.6% ash) and one with pine wood (~0.4 wt% ash), found alkali concentration on the catalyst was around 1 wt% at cumulative biomass to catalyst ratios of around 20 by mass (Figure 1.8). A linear correlation was also found between the concentration of the inorganic species and the Brønsted acidity, suggesting that at least some ion exchange with acidic sites had occurred. This had the effect of decreasing the catalyst activity, both studies report observing increases in bio-oil oxygen content with increasing cumulative biomass to catalyst ratios. Because these catalysts were subjected to high temperatures during

regeneration from coking, physical damage may be another reason for activity loss, as described in more detail hereafter. However, another study specifically looked at the effect of K by preparing ion exchanged catalysts (2.95 wt% loading) and found a drastic reduction in catalyst acidity and yield of aromatic hydrocarbons via CFP of cellulose and switchgrass [59]. The same study also found an increase in furans and phenolics, and the same products are found when catalysts begin to deactivate as a result of coking. Use of *ex situ* CFP methods, whereby the large majority of the inorganic species are removed from the vapor stream with the bio-char, can greatly reduce the impact of this type of deactivation.

In either *in situ* or *ex situ* CFP, however, zeolite catalysts need to be regenerated from coking, likely continuously, if maximized aromatic hydrocarbon production is the goal. Regeneration usually consists of combustion of the coke deposits in an air atmosphere. Because combustion is an exothermic process, it is possible that hot spots may occur during the regeneration processes, making it more likely for catalyst damage to occur. In one study where a commercial spray-dried ZSM-5 catalyst was used in 30 successive reaction/regeneration cycles where the regeneration was performed offline at 580 °C over a long period (15–20 hours), no evidence of dealumination or loss of crystallinity was found, only macroscopic physical damage – some breaking apart of the spray dried particles – was observed [43]. A small loss in performance was attributed to alkali metal poisoning. However, in the aforementioned work using a circulating fluidized bed where the regeneration conditions were much more rapid at measured temperatures of 650–670 °C, evidence of dealumination was evident and a decrease in micropore volumes was observed [42]. The negative effects on performance were limited at 100 hours time on stream, but may become more significant with additional exposure to the reaction/regeneration conditions. Only recently has work been done to optimize the conditions that control temperature during regeneration to prevent catalyst damage. A recent report found that the measured temperature just above a fixed bed regeneration reactor correlated well with the excess of oxygen over the combustion stoichiometry in the atmosphere [60]. Limiting the oxygen to 15 vol% during combustion significantly increased the catalyst lifetime for conversion of furan to aromatics. Further, controlling the temperature via addition of steam further improved the lifetime of the catalyst. This study also explored the idea of a controlled regeneration where a targeted amount of coke remained on the catalyst. Some other processes use this type of partial deactivation (equilibrium state) to control product selectivity, an idea that warrants further study for biomass CFP.

1.1.1.3 Modification of ZSM-5 with Metals

There have been several attempts to modify ZSM-5 to further improve yields, change the selectivity of the products, and/or decrease catalyst deactivation rates. One facile way to modify the zeolite is via ion exchange of the Brønsted acid sites with an active metal cation. There are a few methods to do this, including ion-exchange and incipient wetness impregnation. Some metals can be incorporated into the framework of the zeolite during synthesis. Metals can not only adjust the acidity of ZSM-5 by replacing the proton with a metal cation but also promote desirable reactions during pyrolysis, potentially increasing the yield of

desirable compounds while reducing coke formation on the catalyst. Among the metals that have been studied for this purpose are Zn, Mo, Ga, Ni, Co, Cu, Mn, and Fe [61–75]. Some metal-modified ZSM-5 catalysts are currently being used commercially for the conversion of light hydrocarbons to aromatics. For example, a Ga-modified ZSM-5 catalyst has been used for the aromatization of light alkanes in the Cyclar process by UOP and BP [76–78], while Zn/HZSM-5 is used for the production of aromatics from olefin-rich hydrocarbons in the Alpha process from Asahi Kasei Chemicals Corp. [79]. Modification with gallium has been among the most studied approaches for biomass CFP [43, 56, 68, 70–73]. Gallium incorporation by ion exchange or impregnation has been shown to effect 21–50% increases in yields of aromatic hydrocarbons over parent ZSM-5 catalysts. Catalysts synthesized with Ga in the zeolite framework were less successful for production of aromatics from a model compound (furan) [68]. Table 1.2 summarizes results from various selected CFP studies using GaZSM-5.

The presence of gallium increases the number of Lewis acid sites present in the catalyst, increasing its dehydrogenation activity. Ion exchange methods for preparation of GaZSM-5 have been shown to only effect a minimal amount of actual ion exchange, and much of the gallium exists as Ga_2O_3 on the surface of the catalyst [76]. The small amount of gallium that is exchanged is likely responsible for the increased yields. In a similar process, conversion of ethanol to aromatics, a physical mixture of Ga_2O_3 and HZSM-5 showed no improvement, but the ion exchanged zeolite did [77]. Furthermore, reductive pretreatment appears to mobilize the gallium to ion exchange, further increasing activity. The exchanged Ga(III) sites are most important for the observed activity. The reduction that allows this mobility may not actually perform a reduction to Ga(I) but produce low-coordinate Ga(III) hydride species [77]. Preservation of these states may further enhance the aromatic yield for alkane aromatization reactions.

In CFP, gallium-modified ZSM-5 catalysts that have been prereduced have shown especially strong dehydrogenation activity (as measured by production of H_2), although this rapidly decreases upon exposure to pyrolysis vapors as a result of either oxidation of Ga(I) to Ga(III) or conversion of low coordinate active Ga(III) species to fully ligated species. In either case, the resultant gallium(III)-exchanged catalyst continued to show superior performance for production of aromatic hydrocarbons. The increased dehydrogenation and/or decarbonylation activity afforded increases in olefin formation and in their rate of aromatization. Compared with parent HZSM-5 catalysts, those modified with gallium showed more selectivity toward less alkylated aromatics (benzene and toluene) and away from xylenes [68, 71]. In terms of production of deoxygenated bio-oil, one study of the CFP of pinewood showed a slight increase in yield of organic phase bio-oil (from ~25 to ~26–28 C%) with GaZSM-5 over HZSM-5 with a decrease in oxygen content of the product (from 18.4 to 17.1–17.7 wt%) [73]. Furthermore, GaZSM-5 catalysts have shown longer lifetimes with respect to deactivation due to coking than standard HZSM-5 [56]. Figure 1.9 depicts how GaZSM-5 ($SiO_2/Al_2O_3 = 30$) continued to exhibit superior deoxygenation activity at higher cumulative biomass to catalyst ratios than did its parent HZSM-5 ($SiO_2/Al_2O_3 = 30$) or HZSM-5 ($SiO_2/Al_2O_3 = 80$) during CFP of eucalyptus wood [56].

Table 1.2 Comparison of CFP results for Ga-modified and standard ZSM-5 catalysts.

Catalyst	Biomass	Configuration	SAR[a)]	Temperature (°C)	WHSV[b)](h^{-1})	Bio-oil yield (C%)[c)]/oxygen content (wt%)	AHC[d)] yield (C%)[c)]	References
HZSM-5	Pine	*In situ*	30	550	0.35	—	15.5	[68]
Ga/HZSM-5	Pine	*In situ*	30	550	0.35	—	23.2	
HZSM-5	Pine	*Ex situ*	30	500	7	25.1/18.4	—	[73]
Ga/HZSM-5	Pine	*Ex situ*	30	500	7	28.5/17.1	—	
HZSM-5	Eucalyptus	*In situ*	23	600	C/B = 10	—	14.4	[71]
Ga/ZSM-5	Eucalyptus	*In situ*	23	600	C/B = 10	—	19.7	

a) SAR, silica alumina ratio.
b) WHSV, weight hourly space velocity.
c) C%, carbon yield.
d) AHC, aromatic hydrocarbons.

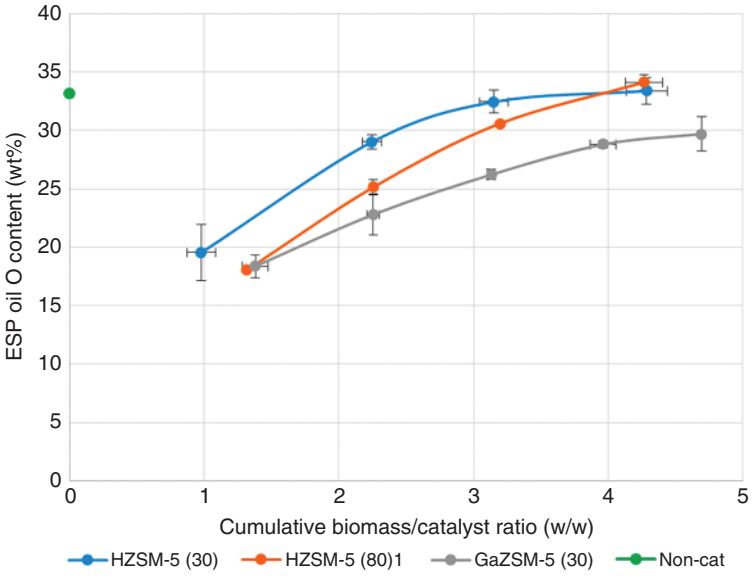

Figure 1.9 Comparison in trend in oxygen content of bio-oil produced via CFP of eucalyptus wood over HZSM-5 ($SiO_2/Al_2O_3 = 30$), HZSM-5 ($SiO_2/Al_2O_3 = 80$) and GaZSM-5 ($SiO_2/Al_2O_3 = 30$), with increasing cumulative exposure of catalysts to biomass. Source: Mullen et al. 2018 [56]. Reproduced with permission of American Chemical Society.

Other metals that have shown positive effects when used to modify ZSM-5 zeolites for CFP are nickel, cobalt, zinc, and iron (Table 1.3) [67, 73–75]. A CoZSM-5 catalyst produced via wet impregnation of ZSM-5 diluted with silica–alumina (for particle size and fluidization properties) was shown to have fewer Brønsted acid sites but greatly increased Lewis acidity. Use of this catalyst produced bio-oil that had lower oxygen content, but at a lower yield than HZSM-5 in a circulating fluidized bed system. The role of the Co was proposed to be similar of that of the Ga [74], i.e. enhancement of dehydrogenation activity to enhance aromatization; however, the reported results with Ga are superior. Nickel has been shown to increase yields of hydrocarbons, up to ~25% over the parent HZSM-5 for conversion of pine wood, a level similar to that of Ga, but the pyrolysis may have to occur in the presence of H_2 for the Ni to retain its activity [73]. The role of Ni seems to be to decrease coke formation, perhaps by hydrogenation. Pyrolysis over NiZSM-5 was more selective for naphthalenes than was HZSM-5 or GaZSM-5. In terms of bio-oil yield and oxygen content, NiZSM-5 produced bio-oil with decreased oxygen content, but with a decreased yield compared with HZSM-5 or GaZSM-5 [73]. Other metals have shown some, but lesser, effects. Iron-modified ZSM-5 has been shown to increase the yield of aromatics in CFP of cellulose and cellobiose (a glucose dimer) compared with HZSM-5, but only at very low Fe loadings where the Brønsted acidity level of the catalyst remained high [67]. Furthermore, the increases noted with isolated carbohydrates did not extend to switchgrass biomass. Fe was shown to change the selectivity toward benzene and naphthalenes and away from production of alkylated benzenes. Other metals have shown little effect on yields but have changed selectivity some; for example, the presence of zinc was shown to increase selectivity for toluene [71].

Table 1.3 Comparison of CFP results for metal-modified and standard ZSM-5 catalysts.

Catalyst	Biomass	Configuration	SAR[a)]	Temperature (°C)	Atmosphere	WHSV[b)](h^{-1})	Bio-oil yield (C%)[c)]/oxygen content (wt%)	AHC yield[d)] (C%)[c)]	References
HZSM-5	Pine	*Ex situ*	30	500	N_2	7	25.1/18.4		[73]
Ni/HZSM-5	Pine	*Ex situ*	30	500	30/70 H_2/N_2	7	24.0/14.4		
Co/HZSM-5	Beech wood	*In situ*		500	N_2	C/B = 12.2	19.9/11.3		[74]
Co/HZSM-5	Beech wood	*In situ*		500	N_2	C/B = 19	16.4/9.8		
HZSM-5	Eucalyptus	*In situ*	23	600	He	C/B = 10	—	14.4	[71]
Zn/HZMS-5	Eucalyptus	*In situ*	23	600	He	C/B = 10	—	12.6	
HZSM-5	Cellulose	*In situ*	23	500	He	C/B = 10	—	14.7	[67]
Fe/HZSM-5	Cellulose	*In situ*	23	500	He	C/B = 10	—	18.0	
HZSM-5	Switchgrass	*In situ*	23	500	He	C/B = 10	–	18.2	
Fe/HZSM-5	Switchgrass	*In situ*	23	500	He	C/B = 10	—	18.3	

a) SAR, silica alumina ratio.
b) WHSV, weight hourly space velocity.
c) C%, carbon yield.
d) AHC, aromatic hydrocarbons.

1.1.1.4 Modifications of ZSM-5 Pore Structure

The microporous structure of the HZSM-5 zeolite is what provides the strong selectivity toward aromatics as well as hinders the diffusion of larger molecules with kinetic diameters >5 Å [25]. These are present in significant quantities in biomass pyrolysis vapor streams. Levoglucosan (6.7 Å) readily undergoes dehydration reactions on the surface of the catalyst to produce molecules smaller than the pore size of HZSM-5; however, lignin-derived guaiacols (~8.1 Å and up) and syringols (~7.9 Å and up) do not have the same reactivity [78, 79]. The poor diffusion of these molecules, and product molecules, contributes to the propensity to form coke, meaning that they are not converted to useful products and also block acid sites, resulting in catalyst deactivation. With this in mind, mesoporous materials, i.e. those with pore sizes of >2 nm, such as SBA-15 or MCM-41, have been well studied for biomass pyrolysis in an effort to overcome the diffusional limitations of the microporous zeolites [26, 80, 81]. However, these materials tend to have weaker and fewer acid sites, can be hydrothermally unstable at biomass pyrolysis conditions, and they lack the selectivity toward aromatics that ZSM-5 exhibits. The result is that these materials tend to promote the dehydration step from carbohydrates resulting in furans, but do not further deoxygenate the latter to the hydrocarbon pool intermediates that are the precursors to aromatics; however, some mesoporous materials have shown increased production of phenols.

There have been efforts to introduce larger pores into zeolitic materials to make mesoporous/microporous materials (possessing what is sometimes referred to as a "hierarchical" pore structure) with the aim of increasing the diffusion rate for bulky materials but preserving the strong acidity and selectivity of the microporous active sites [70, 82–87]. Most of the activity testing on these materials for CFP has been limited to the analytical scale (i.e. micropyrolysis-GC or similar techniques), and selected results are summarized in Table 1.4. The simplest method to produce such materials is to desilicate presynthesized zeolites by treatment with NaOH solutions. Studies using this method have indicated that mild treatment (0.2–0.3 M NaOH at 65–70 °C) of HZSM-5 optimized the catalyst, increasing its performance for the production of aromatic hydrocarbons from wood [82, 83]. Compared with the parent catalysts, the mildly treated catalysts did not show significant variation in elemental composition, crystallographic structure, or microporosity [82]. They did, however, show an increased Brønsted acid site density and increased mesoporosity. More aggressive treatments (using more concentrated NaOH solutions) led to a decrease in micropore volume and decreased performance. Interestingly, two separate studies found that the optimized ZMS-5 catalyst resulted in no change in the aromatic yield and very little change in the selectivity for the CFP of cellulose, but significant increases in aromatic hydrocarbon yield for CFP of beech or red oak wood [82, 83]. This result may indicate improved conversion of bulky lignin-derived substrates with the introduction of mesopores, which is supported by the results of a test using lignin in one of the studies [82].

More recently, some researchers have taken a more systematic approach to synthesizing these hybrid porosity materials in an effort to design an improved catalyst for biomass CFP. Templating techniques to incorporate mesopores

Table 1.4 Comparison of CFP results for ZSM-5 catalysts containing mesopores with standard HZSM-5 catalysts.

Treatment[a)]	Micropore volume (cm^3/g)	Mesopore volume (cm^3/g)	SAR[b)]	Biomass	AHC[c)] yield (C%)	References
None	0.164	0.058	25.5	Cellulose Lignin Beech wood	31.1[d)] 9.89[d)] 23.7[d)]	[82]
0.3 M NaOH	0.133	0.127	24.0	Cellulose Lignin Beech wood	32.1[d)] 13.2[d)] 30.1[d)]	[82]
0.5 M NaOH	0.116	0.210	21.1	Beech wood	26.2[d)]	[82]
None	0.128	0.074	23.2	Cellulose Lignin Red oak	28.5[e)] 11.8[e)] 23.9[e)]	[83]
0.2 M NaOH	0.128	0.123	23.6	Cellulose Lignin Red oak	29.4[e)] 7.7[e)] 27.9[e)]	[83]
0.5 M NaOH	0.110	0.222	26.1	Cellulose	25.3[e)]	[83]
1 M NaOH	0.122	0.174	15.3	Cellulose	25.2[e)]	[83]
None	0.14	0.12	20.3	Cellulose Miscanthus	20.4[f)] 21.8[f)]	[84]
Synthesized	0.12	0.24	9.6	Cellulose Miscanthus	26.1[f)] 24.8[f)]	[84]
None	0.127	—	23	Cellulose	27.5[g)]	[85]
Synthesized	0.113	—	34.4	Cellulose	32.0[g)]	[85]

a) None, commercially sourced HZSM-5; Synthesized, mesoporosity was generated during zeolite synthesis.
b) Silica alumina ratio.
c) AHC = aromatic hydrocarbons (carbon yield).
d) Micropyrolyzer, 550 °C, C/B = 10.
e) Micropyrolyzer, 550 °C, C/B = 20.
f) Micropyrolyzer, 600 °C. C/B = 5.
g) Micropyrolyzer, 700 °C, C/B = 20.

during zeolite synthesis (a bottom-up approach) can offer more control to tailor the properties of the catalysts than washing zeolites with NaOH (a top-down approach) [84]. While some attempts to use bottom-up approaches have had less success than the desilication technique, a combination of techniques has allowed researchers to develop optimized catalysts for CFP. A study using 10 variations in the synthesis of hierarchical mesoporous ZSM-5 led to an optimized catalyst for CFP of cellulose [85]. In addition to the presence of mesopores, high crystallinity was found to be important, as a small concentration of amorphous silica–alumina surface defects was found to impact the diffusion of bulky substrates. The optimized, highly crystalline catalysts improved production of

Table 1.5 Properties of a ZSM-5 catalyst containing mesopores optimized for aromatic hydrocarbon yield via cellulose CFP.

	SAR[a)]	Surface area (m^2/g)			Volume (cm^3/g)		RC[b)]	^{27}Al FWHM[c)] (ppm)	NH_3-TPD BAS peak (°C/area)
		Total	Micro	Meso	Total	Micro			
ZSM-5[d)]	23	372	274	98	0.202	0.127	100	5.9	408/86
ZSM5-OPT	34.4	318	244	74	0.159	0.113	100.7	4.9	432/147

a) Silica-alumina ratio.
b) Relative crystallinity.
c) Framework ^{27}Al NMR signal.
d) Commercial from Zeolyst, CBV2314.
Source: Hoff et al. 2016 [85]. Adapted with permission of John Wiley and Sons.

aromatics from CFP of cellulose by 12%. The reported properties of this catalyst are summarized in Table 1.5 [85]. Another strategy to incorporate mesoporosity is to form nanosheets; the sheets wind up stacked in random orientations, creating a mesoporous/microporous structure [86]. In one study on cellulose CFP using ZSM-5 nanosheets, aromatic hydrocarbon yield was not improved over commercial HZSM-5 using fresh catalysts, but the catalyst lifetime was improved in the case of the nanosheet catalyst due to reduced production of coke [87]. The stability of hybrid materials under regeneration conditions has not yet been explored.

1.1.2 CFP with Metal Oxide Catalysts

Another class of materials receiving considerable attention as potential catalysts for biomass CFP are various forms of metal oxides [88–98]. Metal oxides used for this purpose can be divided into three main groups, namely, acidic metal oxides, basic metal oxides, and transition metal oxides. Some transition metal oxides are being considered for use in reactive catalytic fast pyrolysis (RCFP) processes having a non-inert atmosphere (usually some concentration of H_2). A summary of some typical results of CFP with metal oxide catalysts can be found in Table 1.6.

Acidic metal oxides are somewhat analogous to zeolites in that they promote changes in the pyrolysis pathways via their acid functionality. This class of catalysts includes Lewis acids such as amorphous Al_2O_3, SiO_2, TiO_2, or ZrO_2 [26, 88]. These catalysts are not as effective in the production of oxygen-free hydrocarbons as zeolites, particularly ZSM-5 zeolites; however, bulk reduction of oxygen content through conversion of highly oxygenated species such as anhydrosugars and methoxylated phenols to lesser oxygenated species such as furans, cyclopentenones, and simple phenols is observed. In a large pilot scale study (~1 ton/d) on CFP of loblolly pine, γ-Al_2O_3 was used in a fluidized bed with continuous regeneration of the catalyst from coking. Bio-oil was produced in a yield of 11.5 C% containing 23 wt% oxygen, comparable to some results using HZSM-5 but with lower concentrations of oxygen-free hydrocarbons in the bio-oil [88].

Base metal oxides, particularly MgO and CaO, as well as TiO_2, have long been used in thermal processes for various reasons and have also been studied as

Table 1.6 CFP results using metal oxide and related catalysts.

Catalyst	Biomass	Scale	Configuration	Temperature (°C)	WHSV (h^{-1})	Bio-oil yield (C%)[a]/ oxygen content (wt%)	References
γ-Al_2O_3	Pine	1 Mt/d	*In situ*[b]	520	0.33	11.5/23	[88]
Red mud[c]	Juniper	0.150 kg/h	*In situ*	500	1.5	26.4/25.0	[89]
CaO	Pine	0.060 kg/h	*In situ*[d]	500	C/B = 0.6	22/9.9	[90]
$Ca(COOH)_2$	Pine	0.060 kg/h	*In situ*[d]	500	C/B = 1.4	39/16.3	[90]
MgO	Beech wood	1.5 g batch	*Ex situ*	500	C/B = 0.5	31.6/28.4	[91]
TiO_2	Beech wood	1.5 g batch	*Ex situ*	500	C/B = 0.5	39/35.8	[92]
ZrO_2	Beech wood	1.5 g batch	*Ex situ*	500	C/B = 0.5	39/33.0	[92]
Al_2O_3	Beech wood	1.5 g batch	*Ex situ*	500	C/B = 0.5	23.0/24.0	[92]

a) C%, carbon yield.
b) Catalyst was continuously regenerated.
c) Red mud is a mixture of metal oxides (mainly Fe_2O_3 and Al_2O_3).
d) Catalyst/biomass premixed.

catalysts for biomass CFP. These materials are known catalysts for ketonization and aldol condensation reactions of carboxylic acids and carbonyls [91, 92]. They are therefore able to partially deoxygenate these types of compounds during biomass CFP via these C—C bond forming reactions, releasing CO_2 (as opposed to zeolite catalysis where CO is the main oxygen-carrying gas produced) and H_2O, along with production of new, longer chain ketones. Chain lengthening of small molecules prior to further refining of the bio-oil (e.g. via HDO) is important, so that when the skeletons are deoxygenated the carbon is not lost to gas and is in the correct chain length to operate as a hydrocarbon fuel [91, 92]. Elimination of acids is also a benefit of these reactions. An example of this type of reaction is the conversion of 2 mol of acetic acid (C2) generated via primary pyrolysis reactions to 1 mol of acetone (C3, which can continue to react to larger ketones, including cyclopentenones, under the CFP conditions). In a study of several MgO catalysts for CFP of beech wood, materials with increased porosity and surface area were more effective catalysts [91]. A slightly deoxygenated bio-oil of 28.4 wt% oxygen in about 31% carbon yield was achieved with the most active material screened [91]. Pine wood premixed with CaO was pyrolyzed to produce a highly deoxygenated bio-oil (9.9 wt% oxygen) with a carbon yield of 22 wt% [90]. Use of calcium formate rather than CaO increased the yield; it was suggested that the formate acted as a hydrogen donor, allowing the increase in yield. Elimination of acids and furans was observed, and like the MgO-catalyzed case, an increased production of cyclopentenones was noted. In both cases, increased non-methoxylated phenolic content, particularly *m*-substituted alkyl phenols, was also observed [90, 91]. Subsequent work revealed that both cellulose and lignin were converted to these phenols in the presence of Ca catalysts, but a mechanism for their formation is not known [93]. Similar CFP trends have been reported using TiO_2 and ZrO_2 as well, but with lower performance for deoxygenation [94].

Certain transition metal oxides bring another type of functionality to biomass CFP. Some inspiration for testing these types of catalysts has come from recent success in using molybdenum oxide and molybdenum carbide as effective formulations for the HDO of certain bio-oil model compounds [95, 99–101]. Supported transition metal oxides have been used as effective catalysts for CFP in inert atmospheres or under H_2 at atmospheric pressure (Table 1.7). Various versions of supported molybdenum oxide have been the most successful catalysts in this class found thus far, but some based on iron and tungsten oxides have also been tested. In one study using MoO_3/TiO_2 or MoO_3/ZrO_2 in an *ex situ* CFP method run in a micropyrolysis system under ~70 vol% H_2, a hydrocarbon yield of 27 C% from pine was achieved [96]. This catalyst was much more selective for alkanes (over alkenes and aromatics) than zeolite catalysts, producing these hydrocarbons in a 19 : 2 : 7 ratio, respectively. However, much of the product mixture consisted of small carbon chains with ethane and butane comprising 67–80% of the alkane product. Very high yields of hydrocarbons (C1–C10) via CFP of cellulose and corn stover over prereduced bulk MoO_3 at very high catalyst loadings have also been reported [97]. Another study performed *in situ* CFP using a laboratory scale continuous fluidized bed under H_2 with a supported molybdenum oxide catalyst, yielding 43.2% of highly deoxygenated liquid range bio-oil

Table 1.7 RCFP results using reducible metal oxide catalysts.

Catalyst	Biomass	Configuration	Temperature (°C)	Atmosphere	C/B	Bio-oil yield (C%)[a]/ oxygen content (wt%)	HC yield[b](C%)	References
MoO_3/TiO_2	Pine	*Ex situ*	500	71/29 H_2/He	26		28	[96]
MoO_3/ZrO_2	Pine	*Ex situ*	500	71/29 H_2/He	26		26	[96]
MoO_3	Cellulose	*Ex situ*	500	50/50 H_2/He	~166		72.6	[97]
MoO_3	Lignin	*Ex situ*	500	50/50 H_2/He	~166		35.7	[97]
MoO_3	Corn stover	*Ex situ*	500	50/50 H_2/He	~166		49.5	[97]
W-RMO[c]	Pine	*In situ*	500	N_2		16.9/18.5		[98]
W-RMO[c]	Pine	*In situ*	500	60/40 H_2/N_2		25.0/17.3		[98]
Fe-RMO[c]	Pine	*In situ*	500	N_2		22.0/18.8		[98]
Fe-RMO[c]	Pine	*In situ*	500	60/40 H_2/N_2		36.8/14.8		[98]
Mo-RMO[c]	Pine	*In situ*	450	N_2		26.6/21.4		[98]
Mo-RMO[c]	Pine	*In situ*	450	80/20 H_2/N_2		43.0/6.2		[98]

a) Includes alkanes, alkenes and aromatics including gas and liquid range molecules, carbon yield.
b) Includes products ≥C4, carbon yield.
c) RMO, reducible metal oxide (specific catalyst composition was not disclosed).

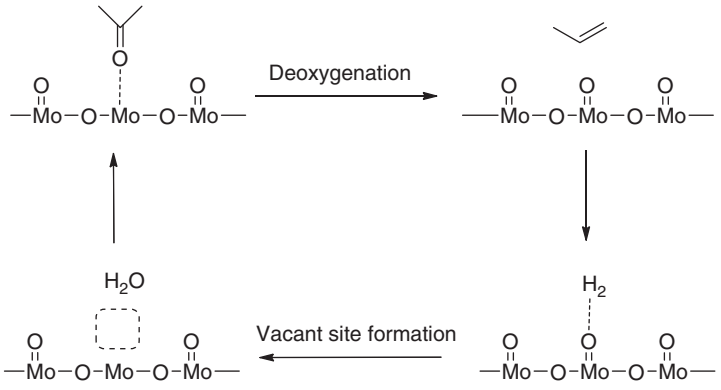

Figure 1.10 Reverse Mars–Van Krevelin mechanism for hydrodeoxygenation (e.g. acetone to propene) over MoO_3. Source: Prasomsri et al. 2013 [101]. Adapted with permission of Royal Society of Chemistry.

product ($\geq C_4$ hydrocarbons, 6.2 wt% oxygen) from pine [98]. The consumption of H_2 during the reaction led to the formation of alkanes and concurrently increased the H/C ratio from what is typically produced from zeolite-catalyzed CFP. The deoxygenation mechanism is thought to be based on oxygen vacancies produced by removal of surface oxygen from MoO_3 via reaction with H_2 to form water. The oxygen vacancies are then filled by removal of oxygen from biomass-derived substrates (a reverse Mars–van Krevelen mechanism, Figure 1.10) [101]. Some deactivation of the catalysts due to coking is observed [96]. Deactivation may also occur due to formation of inactive MoO_2 [96, 97]. Not enough information is yet available to assess how biomass inorganics or exposure to combustion conditions for regeneration would affect the structure of catalysts of this type.

1.1.3 CFP to Produce Fine Chemicals

While complete deoxygenation is desired for fuel purposes, preserving some functionality, and chemical structure of the biomass can lead to the production of more valuable chemical products. Supported Brønsted acids are used as catalysts to perform selective dehydration reactions during pyrolysis. Of particular interest is the direction of cellulose pyrolysis toward levoglucosenone (LGO) rather than levoglucosan (Figure 1.11). LGO is a highly dehydrated sugar monomer that retains one chiral center from cellulose and contains reactive moieties, namely, the alkene double bond and the carbonyl group [102, 103]. This makes it valuable in the preparation of chiral pharmaceutical precursors and for the synthesis of biologically active α,β-unsaturated ketones. The production of LGO from pyrolysis of acid-impregnated cellulose was first reported in 1973, but more recently advances in heterogeneous acid catalysts for these reactions have been made (Table 1.8). These reactions are typically performed at lower temperatures than other CFP processes. One catalyst reported was sulfated zirconia (prepared by impregnation of ZrO_2 with H_2SO_4); at the optimum temperature of 335 °C, the yield of LGO was about 8 wt% from catalytic pyrolysis

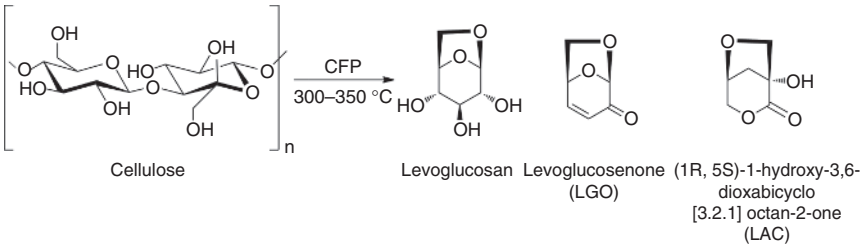

Figure 1.11 Depolymerization and dehydration of cellulose to chiral chemical building blocks via low temperature CFP.

Table 1.8 Low temperature CFP for specific chemicals.

Catalyst[a)]	Biomass	C/B	Temperature (°C)	Targeted product[b)]/ yield (wt%)	References
H_3PO_4	Cellulose	0.03[c)]	335	LGO, 5.6%	[102]
SO_4^{2-}/ZrO_2	Cellulose	1	335	LGO, 8.14%	[102]
SO_4^{2-}/TiO_2-Fe_2O_3	Cellulose	0.33	300	LGO, 15.4	[103]
H_3PO_4/AC	Cellulose	0.33	300	LGO, 18.1	[103]
H_3PO_4/AC	Pine	0.33	300	LGO, 9.1	
H_3PO_4/AC	Poplar	0.33	300	LGO, 8.3	
H_3PO_4/AC	Bagasse	0.33	300	LGO, 6.2	
NP AlTi[d)]	Cellulose	0.3	350	LAC, 8.6	[104]
Pd/SBA-15	Bagasse	0.3	350	4-EG, 0.73	[105]
Pd/SBA-15	Poplar	0.3	350	4-EG, 0.11	
Pd/SBA-15	Pine	0.3	350	4-EG, 0.18	[106]
AC	Bagasse	1.5	300	4-EP, 2.49	

a) AC, activated carbon.
b) LGO, levoglucosenone; LAC, (1*R*, 5*S*)-1-hydroxy-3,6-dioxabicyclo[3.2.1]octan-2-one; 4-EG, 4-ethyl guaiacol; 4-EP, 4-ethyl phenol.
c) Premixed.
d) Nanoparticle Al_2O_3/TiO_2.

of cellulose [102]. Recycling of the catalyst was studied in a limited fashion. Catalysts could be regenerated by combustion of any accumulated char or coke, and the structure of the ZrO_2 support remained intact, but the sulfur content significantly decreased and the support had to be reimpregnated with H_2SO_4 to fully reactivate the catalyst [102]. Similarly, sulfated TiO_2 has also been shown to be effective for this transformation [103]. Another reported catalyst for this transformation was an activated carbon prepared by chemical activation with H_3PO_4 [103]. At 300 °C this catalyst was able to produce LGO in yields of 14.7–18 wt% from cellulose and about 7 wt% from wood. Upon reuse of the catalyst, the yield dropped. Analysis of the spent catalyst indicated a drop in surface area, perhaps from coking [103]. The use of a carbon support is a limitation in this case, as the coke cannot be removed by combustion without destruction of the support.

Another potential chiral synthon from cellulose produced from CFP is (1*R*,5*S*)-1-hydroxy-3,6-dioxabicyclo[3.2.1]octan-2-one (LAC). It was produced in about 8 wt% yield via low temperature (350 °C) pyrolysis of cellulose over nanopowder TiO_2/Al_2O_3 [104]. Further optimization of catalysts for the synthesis of this potentially valuable product has not been reported.

Other targets for biomass catalytic pyrolysis processes include phenols produced by improved selectivity during the decomposition of lignin. Increased yields of 4-ethyl phenol and 4-ethyl guaiacol have been reported for CFP of biomass over Pd on SBA-15, depending on the biomass source [105, 106]. 4-Ethyl phenol appears to form from the net hydrogenation of 4-vinylphenol, a common pyrolytic breakdown product of *p*-hydroxyphenyl (H-type) lignin units, and similarly, 4-ethyl guaiacol is derived from hydrogenation of 4-vinyl guaiacol, derived from G-type lignin units [105]. The hydrogen may be donated from the cellulosic portions of the biomass, as addition of external H_2 is not necessary. An activated carbon catalyst without metal functionality has also been reported for the transformation to ethyl phenol. The best conditions were CFP at a temperature of 300 °C and a catalyst/biomass ratio of 1.5/1, producing 4-ethyl phenol in 2.5 wt% yield from a lignin-enriched bagasse material [106].

1.1.4 Outlook and Conclusions

Zeolite-catalyzed processes for the production of deoxygenated bio-oil as an intermediate to the production of advanced biofuels have received considerable attention from industry. One company, Kior, advanced to the point of running a 500 ton/d plant based on a CFP technology using a proprietary blend of zeolites (including ZSM-5 types) to produce bio-gasoline from pine wood. Kior had planned further expansion and scale-up, but the company went bankrupt in 2014 due to lower than expected product yields [107, 108]. The most complete economic analyses from the US Department of Energy National Renewable Energy Laboratory (DOE NREL) of the zeolite-catalyzed biomass pyrolysis pathway to advanced bio-fuels (including hydrotreatment of the CFP bio-oil) suggests that a price around $3.30 or $3.50/gal of gasoline equivalent for the *in situ* or *ex situ* case, respectively (at biomass cost of $80/ton), is possible at carbon yields of 44% and oxygen content of 6.0–6.4 wt% for the bio-oil intermediate [18]. These targets have not yet been reached in the open literature. The use of biofuel from such a process is estimated to reduce greenhouse gas (GHG) emissions 90% compared with the 2005 petroleum baseline. This reduction in GHG emissions is well above the reduction requirement to be considered as a cellulosic biofuel by the Renewable Fuel Standard (minimum 60% reduction) [18].

While more development is needed to bring CFP of biomass to true economic competiveness with petroleum for production of renewable transportation fuels, one of the appeals of using catalytic pyrolysis is the potential to tailor the pyrolysis process to targeted higher value products over lower margin fuel products. In the realm of zeolite catalysis, one company, Anellotech, is positioning itself to use biomass CFP over zeolites to produce renewable aromatics (particularly BTX: benzene, toluene, xylenes) as a chemical feedstock rather than a fuel feedstock [107] (www.anellotech.com).

As seen in this chapter, other efforts are ongoing to target other high value chemicals, but these are at a much earlier stage in their development than

zeolite-based biomass CFP processes. These other bio-based products may become the economic driver that allow other biomass carbon to find its way to the fuel supply. There is plenty of opportunity for development of not only new and improved catalysts, but of process steps including separation and isolation of targeted products.

References

1 Mohan, D., Pittman, C.U. Jr., and Steel, P.H. (2006). Pyrolysis of wood/biomass for bio-oil: a critical review. *Energy Fuels* 20: 848–889.

2 Huber, G.W., Iborra, S., and Corma, A. (2006). Synthesis of transportation fuels from biomass: chemistry, catalysts, and engineering. *Chem. Rev.* 106: 4044–4098.

3 Meier, D., van del Beld, D., Bridgwater, A.V. et al. (2013). State-of-the-art of fast pyrolysis in IEA bioenergy member countries. *Renewable Sustainable Energy Rev.* 20: 619–641.

4 Weber, K. and Quicker, P. (2018). Properties of biochar. *Fuel* 217: 240–261.

5 Qambrani, N.A., Rahman, M.M., Won, S. et al. (2017). Biochar properties and eco-friendly applications for climate change mitigation, waste management, and wastewater treatment: a review. *Renewable Sustainable Energy Rev.* 79: 255–273.

6 Qian, K., Kumar, A., Zhang, H. et al. (2015). Recent advances in utilization of biochar. *Renewable Sustainable Energy Rev.* 42: 1055–1064.

7 Ensyn Fuels, Inc. (2015). Ensyn, Youngstown Thermal sign RFO biofuel supply agreement, *Biomass Magazine* (08 June), http://biomassmagazine.com/articles/12029/ensyn-youngstown-thermal-sign-rfo-biofuel-supply-agreement.

8 Williams, R.C., Satrio, J., Rover, M.R. et al. (2009). Utilization of fractionated bio oil in asphalt. In: *Transportation Research Board 88th Annual Meeting*. Washington, DC: Transportation Research Board https://trid.trb.org/View/882150.

9 Oasmaa, A., Fonts, I., Pelaaez-Samaniego, M.R. et al. (2016). Pyrolysis oil multiphase behavior and phase stability: a review. *Energy Fuels* 30: 6179–6200.

10 Diebold, J.P. (2000). A Review of the Chemical and Physical Mechanisms of the Storage Stability of Fast Pyrolysis Bio-oils. NREL/SR-570-27613.

11 Baldwin, R.M. and Felik, C.J. (2013). Bio-oil stabilization and upgrading by hot gas filtration. *Energy Fuels* 27: 3224–3238.

12 Elkasabi, Y., Mullen, C.A., and Boateng, A.A. (2014). Distillation and isolation of commodity chemicals from bio-oil made by tail-gas reactive pyrolysis. *ACS Sustainable Chem. Eng.* 2: 2042–2052.

13 Elliott, D.C., Wang, H., French, R. et al. (2014). Hydrocarbon liquid production from biomass via hot-vapor-filtered fast pyrolysis and catalytic hydroprocessing of the bio-oil. *Energy Fuels* 28: 5909–5917.

14 Zacher, A.H., Olarte, M.V., Santosa, D.M. et al. (2104). A review and perspective of recent bio-oil hydrotreating research. *Green Chem.* 16: 491–515.

15 Elliott, D.C., Hart, T.R., Neuenshawander, G.G. et al. (2012). Catalytic hydroprocessing of fast pyrolysis bio-oil from pine sawdust. *Energy Fuels* 26: 3891–3896.
16 Elliott, D.C., Biller, P., Ross, A.B. et al. (2015). Hydrothermal liquefaction of biomass: developments from batch to continuous process. *Bioresour. Technol.* 178: 146–156.
17 Linck, M., Felix, L., Marker, T., and Roberts, M. (2014). Integrated biomass hydropyrolysis and hydrotreating: a brief review. *Wiley Interdiscip. Rev.: Energy Environ.* 3: 575–581.
18 Dutta, A., Sahir, A., Tan, E., et al. (2015). Process Design and Economics for the Conversion of Lignocellulosic Biomass to Hydrocarbon Fuels – Thermochemical Research Pathways with in situ and ex situ Upgrading of Fast Pyrolysis Vapors. NREL/TP-5100-62455.
19 Coombs, D.S., Alberti, A., Armbruster, T. et al. (1998). Recommended nomenclature for zeolite minerals: report of the subcommittee on zeolites of the international mineralogical association, commission on new minerals and mineral names. *Mineral. Mag.* 62: 533–571.
20 Weitkamp, J. (2000). Zeolites and catalysis. *Solid State Ionics* 131: 175–188.
21 Davis, R.J. (2003). New perspectives on basic zeolites as catalysts and catalyst supports. *J. Catal.* 216: 396–405.
22 Mihalcik, D.J., Mullen, C.A., and Boateng, A.A. (2011). Screening acidic zeolites for catalytic fast pyrolysis of biomass and its components. *J. Anal. Appl. Pyrolysis* 90: 197–203.
23 Aho, A., Kumar, N., Eränen, K. et al. (2008). Catalytic pyrolysis of woody biomass in a fluidized bed reactor: influence of the zeolite structure. *Fuel* 87: 2493–2501.
24 Mullen, C.A., Boateng, A.A., Mihalcik, D.J., and Goldberg, N.M. (2011). Catalytic fast pyrolysis of white oak wood in a bubbling fluidized bed. *Energy Fuels* 25: 5444–5451.
25 Jae, J., Tompsett, G.A., Foster, A.J. et al. (2011). Investigation into the shape selectivity of zeolite catalysts for biomass conversion. *J. Catal.* 279: 257–268.
26 Liu, C., Wang, H., Karim, A.M. et al. (2014). Catalytic fast pyrolysis of lignocellulosic biomass. *Chem. Soc. Rev.* 43: 7549–7623.
27 Olsbye, U., Svelle, S., Lillerud, K.P. et al. (2015). The formation and degradation of active species during methanol conversion of protonated zeotype catalysts. *Chem. Soc. Rev.* 44: 7155–7176.
28 Serrano, D.P., Aguado, J., and Escola, J.M. (2012). Developing advanced catalysts for the conversion of polyolefinic waste plastics into fuels and chemicals. *ACS Catal.* 2: 1924–1941.
29 Zhang, H., Cheng, Y.-T., Vispute, T.P. et al. (2011). Catalytic conversion of biomass-derived feedstocks into olefins and aromatics with ZSM-5: the hydrogen to carbon effective ratio. *Energy Environ. Sci.* 4: 2297–2307.
30 Lei, X., Jockusch, S., Ottaviani, M.F., and Turro, N.J. (2003). In situ EPR investigation of the addition of persistent benzyl radicals to acrylates on ZSM-5 zeolites. Direct spectroscopic detection of the initial steps in a supramolecular photopolymerization. *Photochem. Photobiol. Sci.* 2: 1095–1100.

31 Jae, J.H., Tompsett, G.A., Lin, Y. et al. (2010). Depolymerization of lignocellulosic biomass to fuel precursors: maximizing carbon efficiency by combining hydrolysis with pyrolysis. *Energy Environ. Sci.* 3: 358–365.

32 Mullen, C.A. and Boateng, A.A. (2010). Catalytic pyrolysis-GC/MS of lignin from several sources. *Fuel Process. Technol.* 91: 1446–1458.

33 Carlson, T.R., Jae, J., Lin, Y.–.C. et al. (2010). Catalytic fast pyrolysis of glucose with HZSM-5: the combined homogenous and heterogeneous reactions. *J. Catal.* 270: 110–124.

34 Lin, Y.C., Cho, J., Topsett, G.A. et al. (2009). Kinetics and mechanism of cellulose pyrolysis. *J. Phys. Chem. C* 113: 20097–20107.

35 Kawamoto, H., Murayama, M., and Saka, S. (2003). Pyrolysis behavior of levoglucosan as an intermediate in cellulose pyrolysis: polymerization into polysaccharide as a key reaction to carbonized product formation. *J. Wood Sci.* 49: 469–473.

36 Cheng, Y.–.T. and Huber, G.W. (2011). Chemistry of furan conversion into aromatics and olefins over HZSM-5: a model biomass conversion reaction. *ACS Catal.* 1: 611–628.

37 Horne, P.A. and Williams, P.T. (1994). Premium quality fuels and chemicals from the fluidized bed pyrolysis of biomass with zeolite catalyst upgrading. *Renewable Energy* 5: 810–812.

38 Zhang, H., Xaio, R., Huang, H., and Xaio, G. Comparison of non-catalytic and catalytic fast pyrolysis of corncob in a fluidized bed reactor. *Bioresour. Technol.* 100: 1428–1434.

39 Carlson, T.R., Cheng, Y.-T., Jae, J., and Huber, G.W. (2011). Production of green aromatics and olefins by catalytic fast pyrolysis of wood sawdust. *Energy Environ. Sci.* 4: 145–161.

40 Foster, A.J., Jae, J., Cheng, Y.-T. et al. (2012). Optimizing the aromatic yield and distribution from catalytic fast pyrolysis of biomass over ZSM-5. *Appl. Catal., A* 423-424: 154–161.

41 Mullen, C.A. and Boateng, A.A. (2013). Accumulation of inorganic impurities on HZSM-5 zeolites during catalytic fast pyrolysis of switchgrass. *Ind. Eng. Chem. Res.* 52: 17156–17161.

42 Paasikallio, V., Lindfors, C., Kuoppala, E. et al. (2014). Product quality and catalyst deactivation in a four day catalytic fast pyrolysis production run. *Green Chem.* 16: 3549–3559.

43 Jae, J., Coolman, R., Mountziaris, T.J., and Huber, G.W. (2014). Catalytic fast pyrolysis of lignocellulosic biomass in a process development unit with continual catalyst addition and removal. *Chem. Eng. Sci.* 108: 33–46.

44 Wang, K., Kim, K.H., and Brown, R.C. (2014). Catalytic pyrolysis of individual components of lignocellulosic biomass. *Green Chem.* 16: 727–735.

45 Mante, O.D. and Agblevor, F.A. (2014). Catalytic pyrolysis for the production of refinery-ready biocrude oils from six different biomass sources. *Green Chem.* 16: 3364–3377.

46 Karanjkar, P.U., Coolman, R.J., Huber, G.W. et al. (2014). Production of aromatics by catalytic fast pyrolysis of cellulose in a bubbling fluidized bed reactor. *AlChE J.* 60: 1320–1335.

47 Paasikallio, V., Kalogiannis, K., Lappas, A. et al. (2017). Catalytic fast pyrolysis: influencing bio-oil quality with the catalyst-to-biomass ratio. *Energy Technol.* 5: 94–103.

48 Iisa, K., French, R.J., Orton, K.A. et al. (2017). Production of low-oxygen bio-oil via ex situ catalytic fast pyrolysis and hydrotreating. *Fuel* 207: 413–422.

49 Starace, A.K., Black, B.A., Lee, D.D. et al. (2017). Characterization and catalytic upgrading of aqueous stream carbon from catalytic fast pyrolysis of biomass. *ACS Sustainable Chem. Eng.* 5: 11761–11769.

50 Mukarakate, C., Zhang, X., Stanton, A.R. et al. (2014). Real-time monitoring of the deactivation of HZSM-5 during upgrading of pine pyrolysis vapors. *Green Chem.* 16: 1444–1461.

51 Mullen, C.A., Boateng, A.A., Dadson, R.B., and Hashem, F.M. (2014). Biological mineral range effects on biomass conversion to aromatic hydrocarbon via catalytic pyrolysis over HZSM-5. *Energy Fuels* 28: 7014–7024.

52 Wan, S., Waters, C., Stevens, A. et al. (2015). Decoupling HZSM-5 catalyst activity from deactivation during upgrading of pyrolysis oil vapors. *ChemSusChem* 8: 552–559.

53 Hemelsoet, K., Van der Mynsbrugge, J., De Wispelaere, K. et al. (2013). Unraveling the reaction mechanisms governing methanol-to-olefins catalysis by theory and experiment. *ChemPhysChem* 14: 1526–1545.

54 Gayubo, A.G., Aguayo, A.T., Atutxa, A. et al. (2004). Transformation of oxygenate components of biomass pyrolysis oil on a HZSM-5 zeolite. I. Alcohols and phenols. *Ind. Eng. Chem. Res.* 43: 2610–2618.

55 Mullen, C.A., Dorado, C., and Boateng, A.A. (2018). Catalytic co-pyrolysis of switchgrass and polyethylene over HZSM-5: catalyst deactivation and coke formation. *J. Anal. Appl. Pyrolysis* 129: 195–203.

56 Mullen, C.A., Tarves, P.C., Raymundo, L.M. et al. (2018). Fluidized bed catalytic pyrolysis of eucalyptus over HZSM-5: effect of acid density and gallium modification on catalyst deactivation. *Energy Fuels* 32: 1771–1778.

57 Mukarakate, C., McBrayer, J.D., Evans, T.J. et al. (2015). Catalytic fast pyrolysis of biomass: the reactions of water and aromatic intermediates produces phenols. *Green Chem.* 17: 4217–4227.

58 Hoang, T.Q., Zhu, Z., Sooknoi, T. et al. (2010). A comparison of the relativities of propanal and proplylene on HZSM-5. *J. Catal.* 271: 201–208.

59 Mullen, C.A., Tarves, P.C., and Boateng, A.A. (2017). Role of potassium exchange in catalytic pyrolysis of biomass over ZSM-5: formation of alkyl phenols and furans. *ACS Sustainable Chem. Eng.* 5: 2154–2162.

60 Shanshan, S., Zhang, H., Xiao, R. et al. (2018). Controlled regeneration of ZSM-5 catalysts in the combined oxygen and steam atmosphere for catalytic pyrolysis of biomass-derivates. *Energy Convers. Manage.* 155: 175–181.

61 Huber, G.W., Cheng, Y.-T., Carlson, T., et al. (2012). Catalytic Pyrolysis of Solid Biomass and Related Biofuels, Aromatic, and Olefin Compounds. US Patent 8,277,643 B2, filed 3 March, 2009 and issued 2 October 2012.

62 Wang, L., Lei, H., Bu, Q. et al. (2014). Aromatic hydrocarbons production from ex situ catalysis of pyrolysis vapor over zinc modified ZSM-5 in a

packed-bed catalysis coupled with microwave pyrolysis reactor. *Fuel* 129: 78–85.

63 Vichaphund, S., Aht-ong, D., Sricharoenchaikul, V., and Atong, D. (2015). Production of aromatic compounds from catalytic fast pyrolysis of Jatropha residues using metal/HZSM-5 prepared by ion-exchange and impregnation methods. *Renewable Energy* 79: 28–37.

64 Huang, Y., Wei, L., Crandall, Z. et al. (2013). Combining Mo–Cu/HZSM-5 with a two-stage catalytic pyrolysis system for pine sawdust thermal conversion. *Fuel* 150: 656–663.

65 Du, Z., Ma, X., Li, Y. et al. (2013). Production of aromatic hydrocarbons by catalytic pyrolysis of microalgae with zeolites: catalyst screening in a pyroprobe. *Bioresour. Technol.* 139: 397–401.

66 French, R. and Cernik, S. (2010). Catalytic pyrolysis of biomass for biofuels production. *Fuel Process. Technol.* 91: 25–32.

67 Mullen, C.A. and Boateng, A.A. (2015). Production of aromatic hydrocarbons via catalytic pyrolysis of biomass over Fe-modified HZSM5 zeolites. *ACS Sustainable Chem. Eng.* 3: 1623–1631.

68 Cheng, Y.-T., Jae, J., Fan, W., and Huber, G.W. (2012). Production of renewable aromatic hydrocarbons by catalytic fast pyrolysis of lignocellulosic biomass with bifunctional Ga/ZSM-5 catalysts. *Angew. Chem. Int. Ed.* 51: 1387–1390.

69 Park, H.J., Dong, J.I., Jeon, J.K. et al. (2007). Conversion of the pyrolytic vapor of radiata pine over zeolites. *J. Ind. Eng. Chem.* 13: 182–189.

70 Kelkar, S., Saffron, C.M., Li, Z. et al. (2014). Aromatics from biomass pyrolysis vapor using a bifunctional mesoporous catalyst. *Green Chem.* 16: 803–812.

71 Shultz, E.L., Mullen, C.A., and Boateng, A.A. (2017). Aromatic hydrocarbon production from eucalyptus urophylla pyrolysis over several metal-modified ZSM-5 catalysts. *Energy Technol.* 5: 196–204.

72 Kim, J.W., Park, S.H., Jung, J. et al. (2013). Catalytic pyrolysis of mandarin residue from the mandarin juice processing industry. *Bioresour. Technol.* 136: 431–436.

73 Yung, M.M., Stanton, A.R., Iisa, K. et al. (2016). Multiscale evaluation of catalytic upgrading of biomass pyrolysis vapors on Ni- and Ga-modified ZSM-5. *Energy Fuels* 30: 9471–9479.

74 Iliopoulou, E.F., Stefanidis, S., Kalogiannis, K. et al. (2014). Pilot-scale validation of co-ZSM-5 catalyst performance in the catalytic upgrading of biomass pyrolysis vapors. *Green Chem.* 16: 662–674.

75 Yung, M.M., Starace, A.K., Mukarakate, C. et al. (2016). Biomass catalytic pyrolysis on Ni/ZSM-5: effects of nickel pretreatment and loading. *Energy Fuels* 30: 5259–5268.

76 Nowak, I., Quartararo, J., Derouane, E.G., and Védrine, J.C. (2003). Effect of H_2–O_2 pre-treatments on the state of gallium in Ga/H-ZSM-5 propane aromatisation catalysts. *Appl. Catal., A* 251: 107–120.

77 Li, S., Lepore, A.W., Salazar, M.F. et al. (2017). Selective conversion of bio-derived ethanol to renewable BTX over Ga-ZSM-5. *Green Chem.* 19: 4344–4352.

78 Lee, E.H., Park, R., Kim, H. et al. (2016). Hydrodeoxygenation of guaiacol over Pt loaded zeolitic materials. *J. Ind. Eng. Chem.* 27: 18–21.

79 Yu, Y., Li, X., Su, L. et al. (2012). The role of shape selectivity in catalytic fast pyrolysis of lignin with zeolite catalysts. *Appl. Catal., A* 447–448: 115–123.

80 Iliopolou, E.F., Antonakou, E.V., Karakoulia, S.A. et al. (2007). Catalytic conversion of biomass pyrolysis products by mesoporous materials: effect of steam stability and acidity of Al-MCM-41 catalysts. *Chem. Eng. J.* 134: 51–57.

81 Li, Q., Li, W., Zhang, D., and Xi-feng, Z. (2009). Analytical pyrolysis-gas chromatography/mass spectrometry (Py-GC/MS) of sawdust with Al/SBA-15 catalysts. *J. Anal. Appl. Pyrolysis* 84: 131–138.

82 Li, J., Li, X., Zhou, G. et al. (2014). Catalytic fast pyrolysis of biomass with mesoporous ZSM-5 zeolites prepared by desilication with NaOH solutions. *Appl. Catal., A* 470: 115–122.

83 Hoff, T.C., Gardner, D.W., Thiladkaratne, R. et al. (2017). Elucidating the effect of desilication on aluminum-rich ZSM-5 zeolite and its consequences on biomass catalytic fast pyrolysis. *Appl. Catal., A* 529: 68–78.

84 Gamliel, D.P., Cho, H.J., Fan, W., and Valla, J.A. (2016). On the effectiveness of tailored mesoporous MFI zeolites for biomass catalytic fast pyrolysis. *Appl. Catal., A* 522: 109–119.

85 Hoff, T.C., Gardner, D.W., Thilakaratne, R. et al. (2016). Tailoring ZSM-5 zeolites for the fast pyrolysis of biomass to aromatic hydrocarbons. *ChemSusChem* 9: 1473–1482.

86 Lee, H.W., Park, S.H., Jeon, J. et al. (2014). Upgrading of bio-oil derived from biomass constituents over hierarchical unilamellar mesoporous MFI zeolites. *Catal. Today* 232: 119–126.

87 Xu, M., Mukarakate, C., Iisa, K. et al. Deactivation of multilayered MFI nanosheet zeolite during upgrading of biomass pyrolysis vapors. *ACS Sustainable Chem. Eng.* 5: 5477–5484.

88 Mante, O.D., Dayton, D.C., Carpenter, J.R. et al. (2018). Pilot-scale catalytic fast pyrolysis of loblolly pine over γ-Al_2O_3 catalyst. *Fuel* 214: 569–579.

89 Agblevor, F.A., Elliott, D.C., Santosa, D.M. et al. (2016). Red mud catalytic pyrolysis of pinyon juniper and single-stage hydrotreatment of oils. *Energy Fuels* 30: 7947–7958.

90 Case, P.A., Wheeler, M.C., and Desisto, W.J. (2014). Formate assisted pyrolysis of pine sawdust for in-situ oxygen removal and stabilization of bio-oil. *Bioresour. Technol.* 173: 177–184.

91 Stefanidis, S.D., Karakoulia, S.A., Kalogiannis, K.G. et al. (2016). Natural magnesium oxide (MgO) catalysts: a cost-effective sustainable alternative to acid zeolites for the in situ upgrading of biomass fast pyrolysis oil. *Appl. Catal., B* 196: 155–173.

92 Stefanidis, S.D., Kalogiannis, K.G., Iliopulou, E.F. et al. (2011). In-situ upgrading of biomass pyrolysis vapors: catalyst screening on a fixed bed reactor. *Bioresour. Technol.* 102: 8261–8267.

93 Case, P.A., Truong, C., Wheeler, M.C., and DeSisto, W.J. (2015). Calcium-catalyzed pyrolysis of lignocellulosic biomass components. *Bioresour. Technol.* 192: 247–252.

94 Kim, P., Rials, T., Labbé, N., and Chmely, S.C. (2016). Screening of mixed-metal oxide species for catalytic ex situ vapor-phase deoxygenation of cellulose by Py-GC/MS coupled with multivariate analysis. *Energy Fuels* 30: 3167–3174.

95 Nolte, M.W. and Shanks, B.H. (2017). A perspective on catalytic strategies for deoxygenation in biomass pyrolysis. *Energy Technol.* 5: 7–18.

96 Murugappan, K., Mukarakate, C., Budhi, S. et al. (2016). Supported molybdenum oxides as effective catalysts for the catalytic fast pyrolysis of lignocellulosic biomass. *Green Chem.* 18: 5548–5557.

97 Nolte, M.W., Zhang, J., and Shanks, B.H. (2016). Ex situ hydrodeoxygenation in biomass pyrolysis using molybdenum oxide and low pressure hydrogen. *Green Chem.* 18: 134–138.

98 Wang, K., Dayton, D.C., Peters, J.E., and Mante, O.D. (2017). Reactive catalytic fast pyrolysis of biomass to produce high-quality bio-crude. *Green Chem.* 19: 3243–3251.

99 Lee, W., Kumar, A., Wang, Z., and Bhan, A. (2015). Chemical titration and transient kinetic studies of site requirements in Mo_2C-catalyzed vapor phase anisole hydrodeoxygenation. *ACS Catal.* 5: 4104–4114.

100 Sullivan, M.M. and Bhan, A. (2016). Acetone hydrodeoxygenation over bifunctional metallic-acidic molybdenum carbide catalysts. *ACS Catal.* 6: 1145–1152.

101 Prasomsri, T., Nimmanwudipong, T., and Román-Leshkov, Y. (2013). Effective hydroxeoxygenation of biomass-derived oxygenates into unsaturated hydrocarbons by MoO_3 using low H_2 pressures. *Energy Environ. Sci.* 6: 1732–1738.

102 Wang, Z., Lu, Q., Zhu, X., and Zhang, Y. (2011). Catalytic fast pyrolysis of cellulose to prepare levoglucosenone using sulfated zirconia. *ChemSusChem* 4: 79–84.

103 Ye, X., Lu, Q., Wang, X. et al. (2017). Catalytic fast pyrolysis of cellulose and biomass to selectively produce levglucosenone using activated carbon catalyst. *ACS Sustainable Chem. Eng.* 5: 10815–10825.

104 Fabbri, D., Torri, C., and Mancini, I. (2007). Pyrolysis of cellulose catalyzed by nanopowder metal oxides: production and chacterisation of a chiral hydroxylactone and its role as building block. *Green Chem.* 9: 1374–1379.

105 Lu, Q., Zhang, Z., Ye, X. et al. (2017). Selective production of 4-ethyl guaiacol from catalytic fast pyrolysis of softwood biomass using Pd/SBA-15 catalyst. *J. Anal. Appl. Pyrolysis* 123: 237–243.

106 Lu, Q., Ye, X., Zhang, Z. et al. (2016). Catalytic fast pyrolysis of bagasse using activated carbon catalyst to selectively produce 4-ethyl phenol. *Energy Fuels* 30: 10618–10626.

107 Perego, C., Bosetti, A., Ricci, M., and Millini, R. (2017). Zeolite materials for biomass conversion to biofuel. *Energy Fuels* 31: 7721–7733.

108 Adkins, B., Stamires, D., Bartek, R. et al. (2012). Improved catalyst for thermocatalytic conversion of biomass to liquid fuels and chemicals, WO Patent 2012/142490 A1.